03.1

Calibration of heat flux sensors based on anisotropic thermoelements and heterogeneous metal structures using a reflected shock wave

© P.A. Popov, N.A. Monakhov, T.A. Lapushkina, S.A. Poniaev, R.O. Kurakin

Ioffe Institute, St. Petersburg, Russia
E-mail: pavel.popov@mail.ioffe.ru

Received July 6, 2022
Revised August 26, 2022
Accepted August 26, 2022

The applicability of the calibration method for heat flux sensors based on anisotropic bismuth thermoelements and a heterogeneous copper–nickel structure using a reflected shock wave to determine the volt-watt coefficient is demonstrated. The coefficient obtained for a sensor based on anisotropic thermoelements is close to the stationary calibration data, and for a sensor based on a heterogeneous structure, to the results of numerical simulation.

Keywords: heat flux, calibration, shock tube, shock wave, ghfs, hghfs.

DOI: 10.21883/TPL.2022.10.54798.19297

The measurement of the heal flux to the surface of a body is an essential diagnostic tool in a gas-dynamic experiment [1]. Thermoelectric heat flux sensors based on anisotropic bismuth thermoelements (gradient heat flux sensors, GHFSs) and heterogeneous metal structures (heterogeneous gradient heat flux sensors, HGHFSs) have been recently put into practice in experiments with shock tubes. Their operating principle consists in generating a thermoelectric field in a sensing element that exhibits an anisotropic thermal emf when a temperature gradient is induced in it [2]. The results of measurements of the nonstationary heat flux are processed in accordance with the procedures outlined in [3] and [4].

Prior to use, GHFSs and HGHFSs need to be calibrated to determine volt–watt coefficient S_0. A sensor calibrated in stationary thermal conditions is mounted on a special stand and subjected to a heat flux with known density q, and electric signal U is recorded [2]. The sought-for volt–watt coefficient is determined as $S_0 = U/(qA)$, where A is the working surface area. When pulse heat fluxes are measured, it is preferable to perform calibration in nonstationary thermal conditions, which are established using, e.g., a reflected shock wave. This method is relatively easy to implement and is often used for calibration of coaxial thermocouples [5,6]. In the present study, the applicability of this approach in calibration of bismuth GHFSs and copper–nickel HGHFSs is demonstrated. The uncertainty of the obtained volt–watt coefficient depends on the accuracy of measurement of the initial working gas pressure in the low-pressure chamber of a shock tube and the Mach number of an incident shock wave.

The experimental part of calibration is performed in a shock tube. A heat flux sensor and a pressure sensor (triggering the recording system) are mounted at the end of the low-pressure chamber. The theoretical value of heat flux to the wall behind a reflected shock wave is calculated based on the initial experimental data. In the one-dimensional approximation without gas dissociation and ionization and with thermal conductivity $\lambda \sim T^{\nu}$, density $\rho \sim T^{-1}$, and constant thermal capacity C_p, this heat flux may be calculated as [7]

$$q(t) = 1.13\sqrt{\frac{\rho_5\lambda_5 C_5}{2t}}T_5\sqrt{\frac{1-\theta_w^{\nu}}{\nu} - \frac{1-\theta_w^{\nu+1}}{\nu+1}}, \quad (1)$$

where ρ_5, λ_5, and C_5 are the density, the thermal conductivity, and the thermal capacity of gas behind a reflected shock wave; t is time; $\theta_w = T_5/T_w$ is the ratio of the gas temperature behind a reflected shock wave to the wall temperature; and ν is an exponent of power. The heat flux is calculated in accordance with the procedure detailed in [3] based on the experimentally recorded signal of a heat flux sensor and the initial approximation (S_0). It is convenient to use normalized heat flux $q\sqrt{t}$, which depends only on the parameters of gas behind a reflected shock wave, to compare experimental and theoretical data. The value of S_0 is then adjusted so as to minimize the difference in $q\sqrt{t}$ values.

The shock tube of the Ioffe Institute [8] was used a test stand for GHFS and HGHFS calibration. The Mach number of an incident shock wave was determined using piezoelectric pressure sensors mounted at the end of the low-pressure chamber at a distance of 58 mm from each other. Their signals were recorded with a Tektronix TDS 2014 oscilloscope with a time resolution of $4 \cdot 10^{-7}$ s. A GHFS 4×7 mm in size with ten bismuth thermoelements was used in the first series of experiments. Each thermoelement had a length of 7 mm, a width of 0.4 mm, and a thickness of 0.25 mm. According to the stationary calibration data, $S_0 \approx 3.1$ mV/W. The second series of tests was performed for a copper–nickel HGHFS 3×3 mm in size with a thickness of 0.5 mm. The thickness of each metal layer was 0.15 mm. The HGHFS was connected to an INA128P-based amplifier with a gain factor of 200 and a bandwidth of

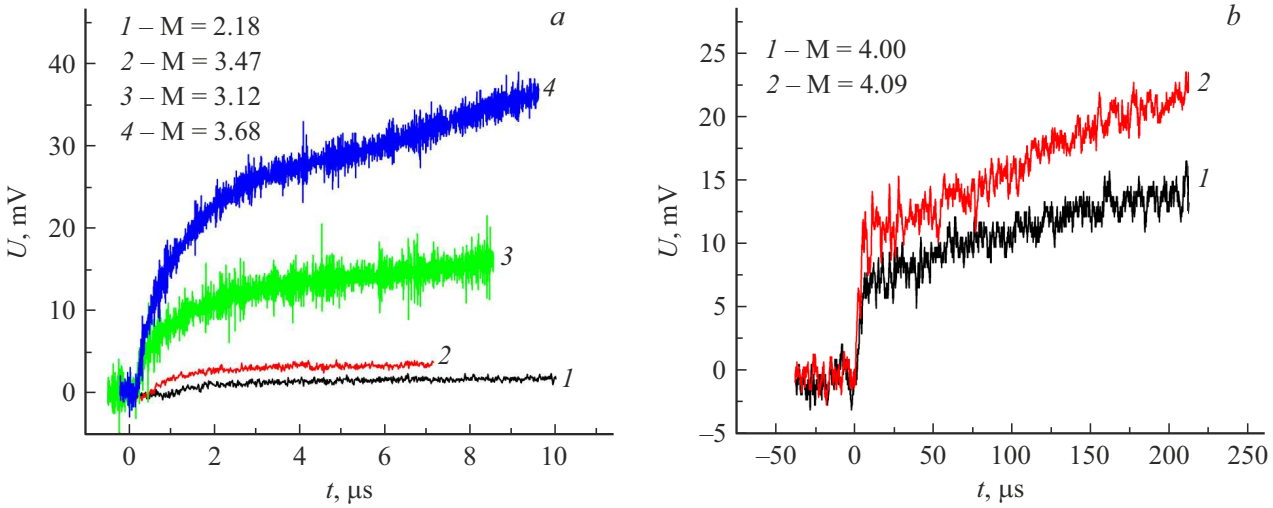

Figure 1. GHFS (a) and HGHFS (b) signals in reflection of a shock wave with different Mach numbers.

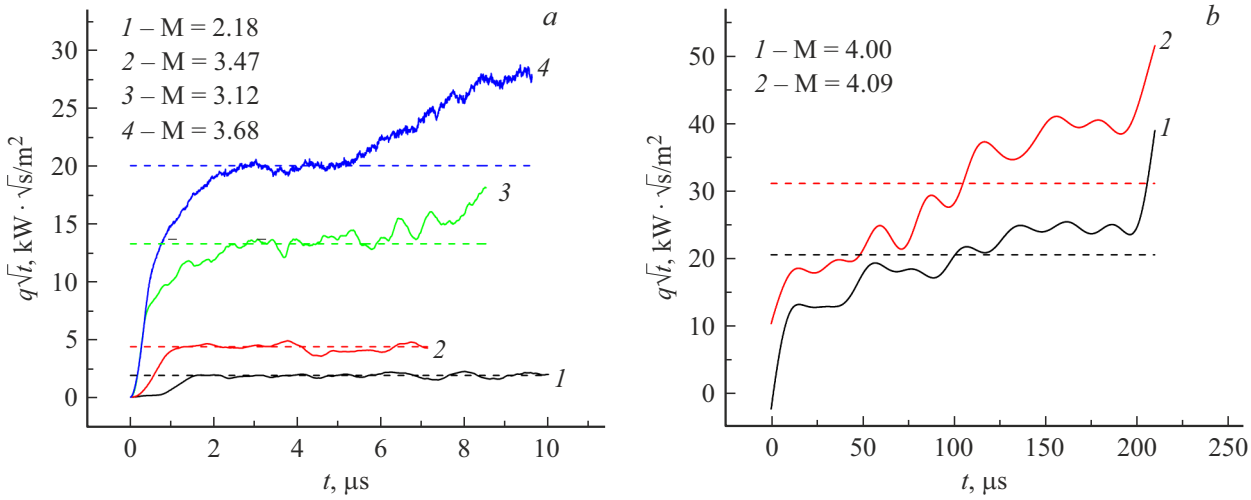

Figure 2. Theoretical normalized heat flux $q\sqrt{t}$ (dashed lines) and heat flux calculated based on GHFS (a) and HGHFS (b) signals for the chosen value of volt–watt coefficient S_0 (solid curves).

~ 200 kHz. The signal from heat flux sensors was recorded with a Tektronix TDS 1002 oscilloscope. The duration of GHFS measurements was $\sim 10\,\mu$s with a time resolution of 10^{-8} s, while the HGHFS measurement duration was $\sim 100\,\mu$s at a resolution of 10^{-7} s.

The volt–watt coefficient of a typical GHFS is $S_0 \sim 1-10$ mV/W, and the coefficient for the considered HGHFS is $S_0 \approx 19\,\mu$V/W (according to the results of calculation in accordance with the model [9] that reproduces the internal sensor structure). Therefore, regimes with different values of normalized heat flux $q\sqrt{t}$ were chosen for GHFS and HGHFS calibration (see the table). Nitrogen served as the working gas in GHFS calibration. In the regimes with Mach number M = 2.18 and 3.47, it also acted as the driver gas; at M = 3.12 and 3.68, it was substituted with hydrogen. Argon was the working gas in HGHFS calibration, while hydrogen was the driver gas.

Figure 1 shows the initial electric GHFS signals (a) and HGHFS signals (b) after amplification. The difference in temperature conductivity of bismuth ($a = 5.5 \cdot 10^{-6}$ m^2/s) and a copper–nickel couple ($a = 5.8 \cdot 10^{-5}$ m^2/s) translates into a difference in temperature distribution within a sensor and, consequently, a difference in signal shape.

Figure 2 shows the theoretical and experimental normalized heat flux values for the GHFS (a) and HGHFS (b) volt–watt coefficient at which the best match of $q\sqrt{t}$ is observed. The initial settling phase of heat exchange with a duration of $\sim 1\,\mu$s and the section of growth of the normalized heat flux were excluded from calculations of the mean $q\sqrt{t}$ value for the GHFS. The initial and end sections with a duration of $\sim 10\,\mu$s, where a considerable $q\sqrt{t}$ variation is observed, were excluded from calculations for the HGHFS. The increase in length of the initial section ignored in averaging for the HGHFS is attributable to the

Initial experimental conditions, calculated parameters of the working gas behind a reflected shock wave, and determined volt–watt coefficient of the sensor

M	P_1, kPa	T_5, K	ρ_5, kg/m^3	C_{p5}, J/(kg · K)	λ_5, W/m · K	$(q\sqrt{t})_{th}$, W · $\sqrt{\text{s}}$/m^2	$\overline{(q\sqrt{t})}_{ex}$, W · $\sqrt{\text{s}}$/m^2	S_0, V/W
GHFS calibration								
2.18	6.67	805	0.552	1123	0.058	1880	1859	$2.9 \cdot 10^{-3}$
3.47	1.33	1607	0.218	1252	0.099	4354	4269	$2.3 \cdot 10^{-3}$
3.12	25.06	1363	3.589	1224	0.088	13247	13053	$2.7 \cdot 10^{-3}$
3.68	19.20	1763	3.362	1267	0.107	20012	19364	$3.9 \cdot 10^{-3}$
HGHFS calibration								
4.00	13.33	3620	1.72	520	0.10011	20664	20008	$15 \cdot 10^{-6}$
4.09	26.66	3779	3.4841	520	0.10291	31244	30557	$15 \cdot 10^{-6}$

fact that the amplifier has a limited bandwidth, and a rapidly increasing signal may thus be distorted. It can be seen that S_0 varies by no more than 20% from one regime to the other (except for M = 3.68) in GHFS calibration. In HGHFS calibration, the same volt–watt coefficient was obtained in two different regimes (see the table).

The behavior of the experimental normalized heat flux in GHFS calibration in the regimes with M = 2.18 and 3.47 follows theoretical predictions throughout the entire time interval. Short sections of steady-state heat exchange following the law of $q \sim 1/\sqrt{t}$ are seen in the regimes with M = 3.12 and 3.68. The duration of these sections decreases with increasing heat flux. The inclusion of such regimes may lead to a considerable error in determination of the GHFS volt–watt coefficient. The $q\sqrt{t}$ curves obtained in HGHFS calibration reveal no steady-state heat exchange phases. Perturbations near the end of the shock tube induced by the interaction between a reflected shock wave and the boundary layer within the considered $\sim 100\,\mu$s time scales are the probable cause here [6]. However, the obtained volt–watt coefficient is still close to the value determined in numerical calculations.

The proper shock tube regimes were selected, and the GHFS and HGHFS calibration was performed with a reflected shock wave to determine the volt–watt coefficient. The use of nitrogen as the working gas in regimes with high normalized heat flux values leads to a suppression of the steady-state heat exchange phase that corresponds to the theoretical dependence. The obtained GHFS volt–watt coefficient is close to the one determined in stationary calibration, and the HGHFS coefficient agrees with the value calculated numerically.

Conflict of interest

The authors declare that they have no conflict of interest.

References

[1] B.R. Hollis, D.K. Prabhu, M. Maclean, A. Dufrene, J. Thermophys. Heat Transf., **31** (3), 712 (2017). DOI: 10.2514/1.T5019

[2] S.Z. Sapozhnikov, V.Yu. Mityakov, A.V. Mityakov, *Heatmetry: the science and practice of heat flux measurement (heat and mass transfer)* (Springer International Publ., 2020).

[3] P.A. Popov, S.V. Bobashev, B.I. Reznikov, V.A. Sakharov, Tech. Phys. Lett., **44** (4), 316 (2018). DOI: 10.1134/S1063785018040235

[4] Yu.V. Dobrov, V.A. Lashkov, I.Ch. Mashek, A.V. Mityakov, V.Yu. Mityakov, S.Z. Sapozhnikov, R.S. Khoronzhuk, Tech. Phys., **66** (2), 229 (2021). DOI: 10.1134/S1063784221020109

[5] B. Birch, D. Buttsworth, F. Zander, Exp. Therm. Fluid Sci., **119**, 110177 (2020). DOI: 10.1016/j.expthermflusci.2020.110177

[6] E. Marineau, H. Hornung, in *Proc. of 47th AIAA Aerospace Sciences Meeting (AIAA)* (Orlando, Florida, 2009), AIAA 2009-737. DOI: 10.2514/6.2009-737

[7] J.A. Fay, N.H. Kemp, J. Fluid Mech., **21** (4), 659 (1965). DOI: 10.1017/S002211206500040X

[8] S.V. Bobashev, A.V. Erofeev, T.A. Lapushkina, S.A. Poniaev, R.V. Vasil'eva, D.M. Van Wie, J. Propuls. Power, **21** (5), 831 (2005). DOI: 10.2514/1.2624

[9] S.V. Bobashev, P.A. Popov, B.I. Reznikov, V.A. Sakharov, Tech. Phys. Lett., **42** (5), 460 (2016). DOI: 10.1134/S1063785016050035